



Synthesis, characterization and kinetic of a surfactant-modified bentonite used to remove As(III) and As(V) from aqueous solution

Jin Su^a, Huai-Guo Huang^b, Xiao-Ying Jin^a, Xiao-Qiao Lu^c, Zu-Liang Chen^{a,*}

^a School of Chemistry and Materials Science, Fujian Normal University, Fuzhou 350007, Fujian Province, China

^b Xiamen Zijin Mining and Metallurgy Technology Co. Ltd., Xiamen 361101, Fujian Province, China

^c Center for Environmental, Sediment and Aquatic Research, Department of Biological Systems Engineering, Washington State University, Pullman, WA 99164-6120, USA

ARTICLE INFO

Article history:

Received 25 March 2010

Received in revised form 30 August 2010

Accepted 31 August 2010

Available online 15 September 2010

Keywords:

Surfactant

Modified bentonite

Adsorption

As(V)

As(III)

ABSTRACT

In this study, organobentonites were prepared by modification of bentonite with various cationic surfactants, and were used to remove As(V) and As(III) from aqueous solution. The results showed that the adsorption capacities of bentonite modified with octadecyl benzyl dimethyl ammonium (SMB3) were 0.288 mg/g for As(V) and 0.102 mg/g for As(III), which were much higher compared to 0.043 and 0.036 mg/g of un-modified bentonite (UB). The adsorption kinetics were fitted well with the pseudo-second-order model with rate constants of 46.7×10^{-3} g/mg h for As(V) and 3.1×10^{-3} g/mg h for As(III), respectively. The maximum adsorption capacity of As(V) derived from the Langmuir equation reached as high as 1.48 mg/g, while the maximum adsorption capacity of As(III) was 0.82 mg/g. The adsorption of As(V) and As(III) was strongly dependent on solution pH. Addition of anions did not impact on As(III) adsorption, while they clearly suppressed adsorption of As(V). In addition, this study also showed that desorb rates were 74.61% for As(V) and 30.32% for As(III), respectively, after regeneration of SMB3 in 0.1 M HCl solution. Furthermore, in order to interpret the proposed adsorption mechanism, both SMB3 and UB were extensively characterized using scanning electron microscopy (SEM), X-ray diffraction (XRD) and Fourier transform infrared (FTIR) analyses.

© 2010 Elsevier B.V. All rights reserved.

1. Introduction

Arsenic is a toxic metalloid element that is considered to be one of the most concerned contaminants in drinking water [1,2]. Soil erosion and leaching contribute to the elevated arsenic either in dissolved species or suspended forms in water [1,2]. In addition, water contamination by arsenic also results from discharge of mining industry wastewater into aquatic environment [2,3]. Methods for arsenic removal from drinking water currently include precipitation/co-precipitation, filtration, adsorption, ion exchange, membrane dialysis, and biomass remediation [1,2,4].

Development of novel adsorbents generally involves in new technology for arsenic removal [2]. Various materials such as zeolites [3,5,6], clays [7–11], activated carbon [12], biomaterials [13], metal oxides [14], zero-valent iron [15] and neutralized red mud [16] have been used as adsorbents to remove arsenic from contaminated and waste water. Among them, clays, due to their inexpensive, acceptability, applicability, abundance and high adsorption efficiency, have been received much attention in removal of heavy metals from contaminated water [17]. Bentonite

modified either with Fe, Al, or Mn salts showed significant improvements in adsorption affinity for arsenic, by which the removal percents of As(III) ranged from 92% to >99% with the corresponding adsorption capacity up to 4.5 mg/g [7]. Montmorillonite modified with polymeric Al/Fe was used to adsorb As(III), As(V) and dimethylarsinate (DMA) from aqueous solutions, where the maximum adsorption capacity of the adsorbent was obtained in the pH range from 3.0 to 6.0 for As(V), 7.0 to 9.0 for As(III) and 3.0 to 7.0 for DMA [8]. Kolinite modified with humic acids could adsorb As(V) more effectively than un-modified kaolinite at pH 7.0 [9]. Clay pillared with titanium(IV), iron(III) and aluminum(III) showed similar adsorption capacities for As(V) but differences in adsorption capacities for As(III) [10].

Recently, arsenic adsorption on the raw clay modified with cationic surfactants has been received much more attention. The organoclays are prepared by exchange of Na⁺ or Ca²⁺ cations with cationic surfactants participated on the surfaces of clays, where charge on the clay surface is reversed from negative to positive [18]. The positively charged head groups are balanced by counteranions (A⁻), which makes the raw clay modified with cationic surfactants to be a potential adsorbent to adsorb anionic contaminants, such as arsenate oxyanions, via ion exchange mechanism [3,5,11,18]. Li and Bowman [11] used kaolinite intercalated with hexadecyltrimethylammonium bromide (HDTMA) as an effective

* Corresponding author. Tel.: +86 (591) 83465689; fax: +86 (591) 83465689.
E-mail address: zlchen@fjnu.edu.cn (Z.-L. Chen).

adsorbent for arsenate removal, and reported that adsorption capacity of As(V) onto the organo-kaolinite was at least two magnitudes greater than un-modified kaolinite. Though kaolinite and zeolite modified by HDTMA enhanced As(V) adsorption significantly, only a minor increase in As(III) adsorption. This is because the adsorption mechanism for As(V) is through surface anion exchange, while adsorption mechanism for As(III) may involve in surface complexation [18].

Nevertheless, little work on raw bentonite modified with cationic surfactants as adsorbents for removal of arsenic from aqueous solution has been reported. The aims of this study were to use bentonite modified by a cationic surfactant for the removal of As(V) and As(III) from aqueous solution. Adsorption behaviors of As(V) and As(III) on the modified bentonite by different cationic surfactants were compared. In order to understand possible mechanism of adsorption, effects of experimental conditions such as contact time, solution pH, initial concentration, pH, ionic strength and addition of anion on adsorption of As(V) and As(III) were investigated. Kinetics and isotherms of adsorption of As(V) and As(III) on the organobentonite, and its regeneration of the adsorbent was also studied. In addition, the characterization of modified and un-modified bentonite using EMS, XRD and FTIR spectroscopic techniques was conducted.

2. Theories of adsorption

2.1. Adsorption performance

The adsorption capacity of arsenic by the adsorbent was calculated by difference in concentrations using the following equation:

$$Q_t \text{ (mg/g)} = \frac{(C_0 - C_t) \cdot V/1000}{W} \quad (1)$$

where Q_t is the adsorption capacity of arsenic on the adsorbent at time t , C_0 is the initial arsenic concentration (mg/L), C_t is the concentration of arsenic in solution at time t (mg/L), V is the volume of arsenic solution used (mL), and W is the mass of the adsorbent used (g).

2.2. Adsorption kinetics

The pseudo-second-order kinetic model was used to describe the adsorption process. It is expressed using the following equation [19]:

$$\frac{t}{Q_t} = \frac{1}{(k_2 Q_2^2)} + \frac{t}{Q_2} \quad (2)$$

where Q_2 is the maximum adsorption capacity (mg/g) of arsenic on the adsorbent, Q_t (mg/g) is the adsorption capacity at equilibrium time and at time t (h), and k_2 (g/(mg h)) is the rate constant of adsorption. Values of k_2 and Q_2 can be calculated from the plot of t/Q_t against t . The initial adsorption rate constant h (mg/(g h)) can be obtained according to the following equation:

$$h = k_2 \times Q_2^2 \quad (3)$$

2.3. Adsorption isotherms

Adsorption isotherms were used to understand the adsorption interaction and to design adsorption systems. Most of the adsorption data can be expressed in the Langmuir and the Freundlich models. The Langmuir isotherm is expressed using the following equation [20]:

$$\frac{1}{Q_e} = \frac{1}{Q_m} + \frac{1}{Q_m K_L C_e} \quad (4)$$

where Q_e (mg/g) is the adsorption capacity at equilibrium time t ; Q_m (mg/g) is the maximum adsorption capacity; C_e (mg/L) is the equilibrium concentration of arsenic and K_L (L/mg) is a constant related to the adsorption energy.

Based on the further analysis of the Langmuir equation, the dimension parameter of the equilibrium or adsorption intensity (R_L) can be expressed using the following equation [21]:

$$R_L = \frac{1}{(1 + K_L C_0)} \quad (5)$$

where C_0 (mg/L) is the initial concentration of arsenic. The parameter R_L is considered as an indicator of adsorption. The values of R_L indicate the type of the isotherms: $R_L > 1$ for unfavorable adsorption; $R_L = 1$ for linear adsorption; $0 < R_L < 1$ for favorable adsorption; $R_L = 0$ for irreversible adsorption.

The Freundlich isotherm model is an empirical equation, which is valid for an adsorption that is assumed that process occurs between the concentrations of a solute on the heterogeneous surface of an adsorbent and the solute in the liquid. The Freundlich isotherm is expressed using the following equation [22]:

$$\ln Q_e = \ln K_F + \frac{1}{n} \ln C_e \quad (6)$$

where K_F and n are the Freundlich constants that are associated with the relative capacity and adsorption intensity, respectively.

Thermodynamic parameters such as standard Gibbs free energy change (ΔG°) can be calculated using the following equation [6]:

$$\ln(K_F \times 1000) = -\frac{\Delta G^\circ}{RT} \quad (7)$$

where K_F is the Freundlich constants, given in Eq. (6), R is universal gas constant (8.314 J/mol K), and T is the absolute temperature.

3. Materials and methods

3.1. Preparation of organobentonite

The bentonite used in this study was supplied by Fenghong Co. Ltd., Jian, Zhejiang, China. The cation exchange capacity (CEC) measured was 75.4 mequi/100 g. The chemical composition of the bentonite was 62.5% SiO₂, 18.5% Al₂O₃, 1.75% Fe₂O₃, 4.25% MgO, 0.95% CaO, and 2.75% Na₂O. The surfactants used for modification were octadecyl trimethylammonium chloride (OTMA), octadecyl benzyl dimethylammonium chloride (OBDMA), and diocadecyl dimethylammonium chloride (DODMA). Na₂HAsO₄·7H₂O and NaAsO₂ were of analytical reagent grade and used without further purification. The pH of experimental solution was adjusted using 0.01 M solutions of NaOH or HCl.

SMB3 was prepared in the following procedure. Briefly, 1.5 g of the bentonite was initially dispersed into deionized water and stirred with a magnetic stirrer at 600 rpm for 3 h and was then mixed with the cationic surfactant solution (1.1 CEC). The mixture was stirred slightly in order to avoid frothing in water bath at 80 °C for 1.5 h. The ratio of water to the bentonite was 20. The suspension was subsequently washed with deionized water 4 times. The moist solid material was dried in an oven at 60 °C and ground using a pre-washed mortar and pestle. The montmorillonite content in the organobentonite ranged from 96% to 98% with the measured diameter less than 75 μm, lamellar distance less than 2.5 nm, and apparent density less than 0.30 g/cm³.

3.2. Characterization

Solid morphological characteristics of UB and SMB3 were analyzed using a scanning electron microscopy (SEM) (JSM 7500F, Japan). The crystal textures of UB and SMB3 were determined using an X-ray diffraction (XRD) instrument (X' Pert Pro MPD, Holland) with filtered Cu Kα radiation operated at 40 kV and 40 mA.

The XRD pattern was recorded from 1.5° to 30° of 2θ with a scanning speed of 0.02° of 2θ per second. Infrared spectra of UB and SMB3 were obtained using a Fourier transform infrared (FTIR) spectrometer (FTIR Nicolet 5700, Thermo Corp., U.S.A.). Samples for FTIR measurement were prepared by mixing 1% (w/w) of specimens with 100 mg of KBr powder and pressing the mixture into a sheer slice. An average over 9 scans was collected for each measurement with a resolution of 2 cm^{-1} .

3.3. Adsorption experiments

1 g of the adsorbent was added into 100 mL of 0.01 M NaCl solution (background electrolyte) with desirable concentrations of As(V) and As(III) in a 250 mL conical flask. The flask was shaken on a shaker at $33 \pm 1^\circ\text{C}$. Various experimental conditions, including contact time (10–600 min), pH (2–11), ionic strength (0–0.5 M), major anion (chloride, sulfate, fluoride and phosphate) and initial concentrations (0.2–60 mg/L), were tested. After filtration, As(V) and As(III) concentrations in the aqueous phase were determined using a PE2100DV ICP-OES instrument. Blank control tests without any adsorbent were carried out in parallel. All experiments were carried out in duplicates.

The efficiencies of arsenic adsorption on different adsorbents were studied at $33 \pm 1^\circ\text{C}$ with a solution containing 5 mg/L of As(V) and As(III), 0.01 M NaCl, at initial pH, and contact time of 6 h for As(III) and 8 h for As(V).

The effect of contact time on arsenic adsorption was studied at $33 \pm 1^\circ\text{C}$ with a solution containing 5 mg/L of As(V) and As(III), 0.01 M NaCl, at initial pH.

The effect of initial concentration on arsenic adsorption was studied at $33 \pm 1^\circ\text{C}$ with a solution containing different concentrations of As(V) and As(III), ranging from 0.2 to 50 mg/L, 0.01 M NaCl, at initial pH, and contact time of 6 h for As(III) and 8 h for As(V).

The effect of pH on arsenic adsorption was investigated in the pH ranges from 2 to 11 at $33 \pm 1^\circ\text{C}$ with a solution containing 5 mg/L of As(V) and As(III), 0.01 M NaCl, and contact time of 6 h for As(III) and 8 h for As(V).

The effect of ionic strength on arsenic adsorption was investigated in the ionic strength ranges of 0–0.5 M at $33 \pm 1^\circ\text{C}$ with a solution containing 5 mg/L of As(V) and As(III), at initial pH, and contact time of 6 h for As(III) and 8 h for As(V).

The effect of addition anions with 0.01 M of chloride, sulfate, fluoride and phosphate on arsenic adsorption was investigated at $33 \pm 1^\circ\text{C}$ with a solution containing 5 mg/L of As(V) and As(III), at initial pH, and contact time of 6 h for As(III) and 8 h for As(V).

3.4. The determination of pH_{pzc}

The batch equilibrium experiments were used to estimate the point of pH_{pzc} . For this, 0.2 g of adsorbent was added into 100 mL 0.01 M NaCl solution (background electrolyte). The initial pH ($\text{pH}_{\text{initial}}$) were adjusted the values ranging from 2 to 12 by adding minimum amounts of 0.01 M NaOH or 0.01 M HCl. The suspensions were equilibrated for 24 h in a rotary shaker at 200 rpm at room temperature. The suspensions were filtered and final pH values (pH_{final}) of the filtrates were re-measured. A plot of the final pH as a function of the initial pH provides pH_{pzc} of the adsorbents by the plateau of constant pH to the ordinate.

4. Results and discussion

4.1. Efficiency of arsenic adsorption on different adsorbents

As shown in Fig. 1, the adsorption capacities of As(V) are 0.189, 0.112 and 0.288 mg/g, while the corresponding values of As(III)

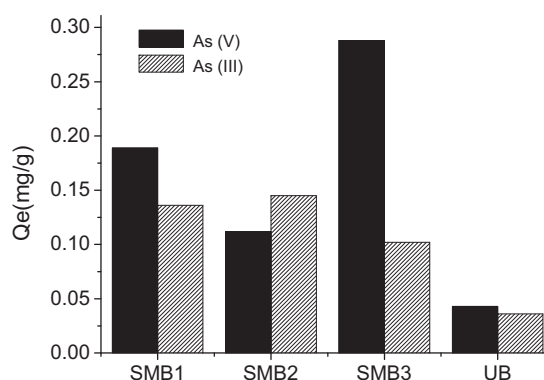


Fig. 1. Efficiency of As(V) and As(III) adsorption on different sorbents. Dose: 10 g/L; background electrolyte: 0.01 M NaCl; pH: initial pH (8.86); equilibration time: 6 h for As(III) and 8 h for As(V); rotary speed: 250 rpm, initial concentration: 5 mg/L and temperature: $33 \pm 1^\circ\text{C}$.

are 0.136, 0.145 and 0.102 for SMB1, SMB2 and SMB3, respectively. The results showed that the modified organobentonite had a much higher adsorption capacity for arsenate compared to UB (0.036 for As(III) and 0.043 for As(V)), and the species of quaternary ammonium salt had more influence on adsorption of As(V) than on adsorption of As(III). This may be because of that the adsorption of As(V) is through anion exchange that has been well verified and discussed by some other researchers [3,11,18]. The benzyl conjugate effect of SMB3 could lead to a deviate from its molecular structure, resulting in that the exchange of chloride ions occurs more easily. While surface anion exchange is not a major mechanism for As(III) adsorption [18], adsorption of As(III) may be mainly a physical adsorption. The adsorption capacities of As(V) obtained were in the order: SMB3 > SMB1 > SMB2, while the adsorption capacities of As(III) were in the order: SMB2 > SMB1 > SMB3. As shown in Table 1, the different basal spacing of organobentonite samples obtained is due to the modification by different cationic surfactants. Consequently, the different adsorption capacities for As(V) and As(III) were obtained due to the different sizes of the surfactant molecules. In this case, hence, SMB3 was used in the further experiments.

4.2. Characterization of SMB3

Fig. 2(a) and (b) shows the ESM images of bentonite before and after modification. The ESM image of UB (Fig. 2(a)) shows the surface contexture is not smooth but granule alike with an anomalous character. In comparison, the ESM image of SMB3 (Fig. 2(b)) shows that the surface architecture is much smoother, characterized with smaller size fragments and sheet alike contexture, indicating that bentonite may be homogeneously dispersed throughout modification of the surfactant.

Fig. 3(a) and (b) shows the XRD patterns of UB and SMB3. The basal spacing of UB measured was 1.26 nm, representing a typical XRD pattern of Na-bentonite with the $d(001)$ plane reflection peak at about 6° , which corresponds to the basal spacing with coordinating Na^+ and Ca^{2+} ions in the interlayer space with one molecular water layer (1.34 nm) [23]. However, as for SMB3, the basal spacing increased to 3.11 nm with modification of the surfactant. This

Table 1
The XRD $d(001)$ of bentonites modified with different surfactants.

Sample	Surfactant	XRD $d(001)$
SMB1	OTMA	~2.2 nm
SMB2	DODMA	~3.6–3.7 nm
SMB3	OBDMA	~3.11 nm
UB		1.26 nm

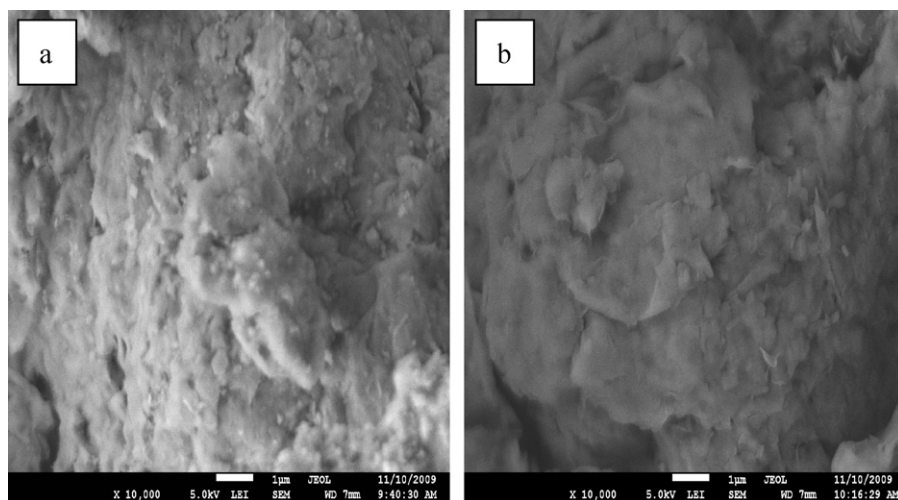


Fig. 2. SEM images of UB (a) and SMB3 (b).

is attributed to the surfactant molecular arrangement laying flat in the interlayer space, leading to expansion of the interlayer space [23,24]. As listed in Table 1, the result shows that the basal spacing of SMB1 and SMB2 increases to 2.2 and 3.6–3.7 nm, respectively due to the different sizes of the surfactant molecules. The thickness of montmorillonite layer is 0.96 nm, while the height of alkyl chain lying parallel to the clay layer ranges between 0.4 and 0.45 nm, depending on its orientation. The basal spacing suggests either a coexistence of bilayer or pseudotrimolecular arrangements of the intercalated surfactant.

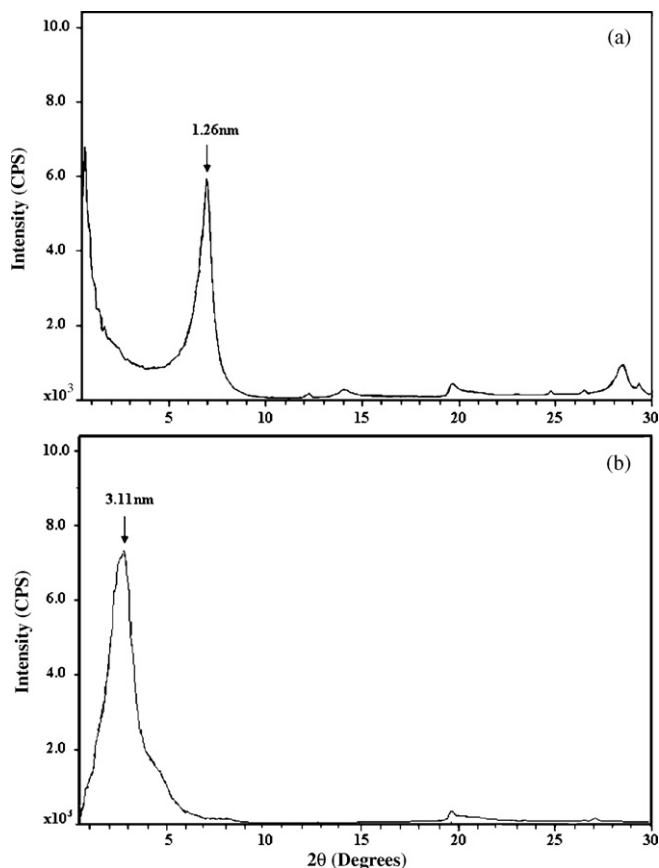


Fig. 3. XRD patterns of UB (a) and SMB3 (b).

Fig. 4(a) and (b) shows the FTIR spectra of UB and SMB3 recorded in the wave numbers ranging from 400 to 3500 cm^{-1} . The bands of UB at 1041 and 915 cm^{-1} represent the bending vibrations of Si–O and Al–O, respectively [23,25]. The bands at 464, 519 and 3627.5 cm^{-1} are due to the stretching vibrations of Al–O–Si and OH groups in bentonite. The bands at 1467.28 and 1486.77 cm^{-1} correspond to ammonium ions, suggesting that the composition of the organobentonite in the interlayer space may undergo ion exchange of Na^+ by NH_4^+ ion. The bands at 2922.53 and 2852.28 cm^{-1} are due to the stretching vibrations of symmetric and antisymmetric CH_2 [26]. The band at 1640.38 cm^{-1} corresponds to water bending modes within the interlayer of bentonite. The intensity of this band after modification decreased, indicating loss of water. Nevertheless, most bands are identical after modification by the surfactant, suggesting that the core crystal structure of UB and SMB3 remains. In summary, results obtained from SEM, FTIR and XRD measurements provide the clear evidences that the surfactant is incorporated into the interlayer of bentonite, which support the adsorption mechanism for As(V) to be mainly through anion exchange, and for As(III) to undergo surface adsorption [18].

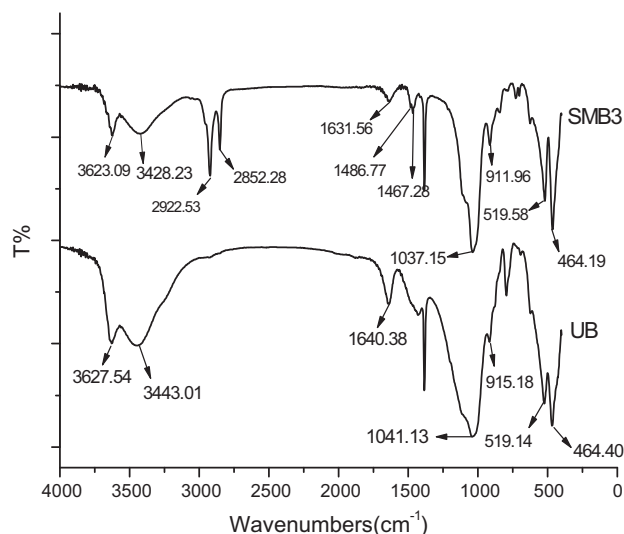


Fig. 4. FTIR spectra of UB and SMB3.

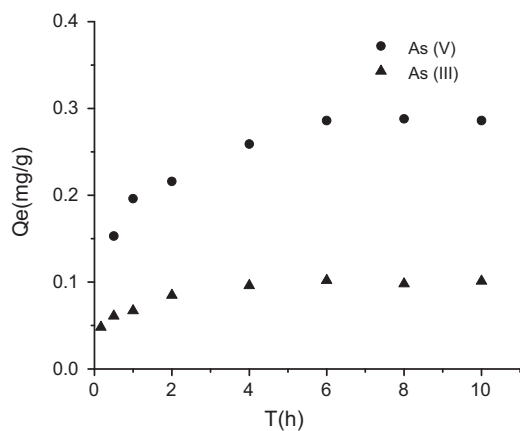


Fig. 5. Effect of contact time on As(V) and As(III) adsorption by SMB3. Dose: 10 g/L; background electrolyte: 0.01 M NaCl; pH: initial pH (8.86); rotary speed: 250 rpm, initial concentration: 5 mg/L and temperature: $33 \pm 1^\circ\text{C}$.

4.3. Effect of contact time on arsenic adsorption

The effects of the contact time on adsorption of As(V) and As(III) on SMB3 are shown in Fig. 5. The adsorption capacities at the equilibrium were 0.288 mg/g for As(V) and 0.102 mg/g for As(III), respectively. The adsorption was fast within the first 30 min and reached equilibrium within 4 h for As(III) and 6 h for As(V). The contact time of 6 h for As(III) and 8 h for As(V) were used in the following experiments to ensure a maximum adsorption. Initial adsorption rates were high for both As(V) and As(III). This is due to the fact that sticking probability is high in the initial external surface [3,6]. The active sites are gradually filled up as adsorption progresses, leading to that adsorption rate becomes slow when the kinetics is dependent on the rate associated with intraparticle diffusion. The equilibrium time of As(III) was less than As(V). This may be due to the different adsorption mechanism between As(V) and As(III). As shown in Fig. 6, the correlation coefficients of R^2 , 0.9983 for As(V) and 0.9984 for As(III), are obtained from the pseudo-second-order kinetic model, respectively. This suggests that the pseudo-second-order model is fitted well to describe the adsorption behaviors of As(V) and As(III) on SMB3, indicating that the adsorption process might be chemisorption [8]. Previous studies also reported that the pseudo-second-order model was correlated well with the experimental data on the adsorption of arsenic on the clay materials that were similarly modified [8,12,27]. The pseudo-second-order rate constants (K) were $46.7 \times 10^{-3} \text{ g/mg h}$ for As(V) and $3.1 \times 10^{-3} \text{ g/mg h}$ for As(III), respectively. In addition, the ini-

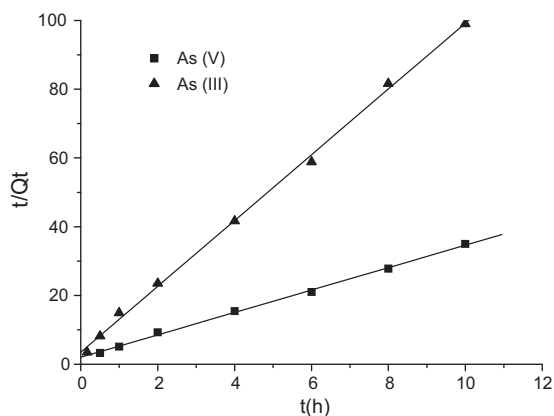


Fig. 6. The pseudo-second-order kinetic model of As(V) and As(III) adsorption by SMB3.

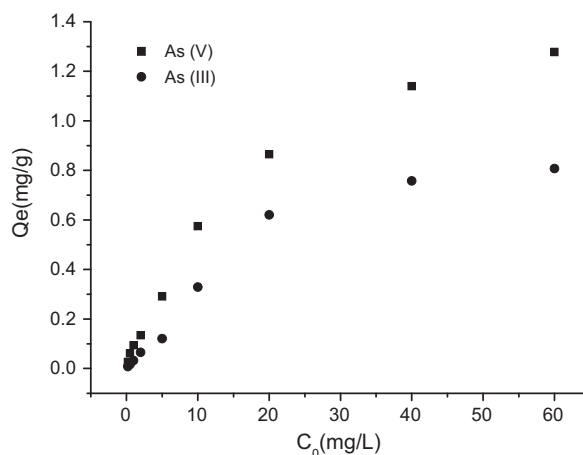


Fig. 7. Effect of initial concentration on As(V) and As(III) adsorption by SMB3. Dose: 10 g/L; background electrolyte: 0.01 M NaCl; pH: initial pH (8.86); equilibration time: 6 h As(III) for and 8 h for As(V); rotary speed: 250 rpm and temperature: $33 \pm 1^\circ\text{C}$.

tial adsorption rate constant were $4.4 \times 10^{-3} \text{ mg/g h}^{-1}$ for As(V) and $3.38 \times 10^{-5} \text{ mg/g h}^{-1}$ for As(III). This indicates that the adsorption rate constant of As(III) is smaller than As(V).

4.4. Effect of initial concentration on arsenic adsorption

The maximum level of arsenic concentration in public drinking water has been dropped from 50 ppb (0.05 mg/L) to 10 ppb (0.01 mg/L) in China recently. Although some adsorbents show good efficiencies in removing arsenic from water containing high concentration of arsenic, they probably are not good enough to remove arsenic from water down to ppb levels [12,28,29]. Therefore, it is very important to develop an adsorbent that can remove arsenic from water down to 10 ppb. Fig. 7 shows changes in the equilibrium adsorption capacities of arsenic as a function of initial concentrations. As(V) concentrations were reduced from initial concentrations of 0.2, 0.5 and 1.0 mg/L to 0.0037, 0.0073, and 0.04 mg/L after being treated with SMB3, indicating that SMB3 could remove arsenic either down to level of 0.01 mg/L or to 0.05 mg/L, depending on the initial concentration of As(V). However, in comparison, the final concentrations of As(III) were all above 0.05 mg/L when the corresponding initial concentrations were used. Therefore, the SMB3 is not capable to remove As(III) efficiently even down to the maximum level of 0.05 mg/L.

Table 2 summarizes the constants of the Langmuir and Freundlich adsorption isotherms of arsenic adsorption on SMB3, where most of correlation coefficient (R^2) values exceed 0.9 derived from both the Langmuir and Freundlich models, suggesting that both models fit well with the experimental results. The maximum adsorption capacities (Q_m) calculated from the Langmuir were 1.48 mg/g for As(V) and 0.82 mg/g for As(III), respectively. Although it was found that the adsorption capacity for arsenic adsorption onto SMB3 lower than those for other adsorbents (Table 3), SMB3 shows a good capability of removing arsenic from water down to ppb levels, making the adsorbent to be used commercially in

Table 2

The constants of the Langmuir and Freundlich adsorption isotherms of adsorption of arsenic on SMB3.

	Freundlich isotherm			Langmuir isotherm		
	K_F	$1/n$	R^2	Q_m (mg/g)	K_L (L/mg)	R^2
As(V)	0.18	0.56	0.941	1.48	0.11	0.998
As(III)	0.04	0.81	0.968	0.82	0.07	0.957

Table 3
Comparison of maximum sorption capacity with other adsorbents.

Adsorbent	Adsorption capacity (mg/g)		References
	As(III)	As(V)	
SMNM		7.29	[3]
SMNC		3.40	[3]
SMZY-100-S		17.89	[5]
H24		35.8	[6]
BT-FeIII	0.1		[7]
Al/Fe modified montmorillonite	19.11	21.23	[8]
Acid modified carbon black		46.3	[12]
HDTMA modified kaolinite	0.32	0.67	[18]
Zr(IV)-loaded SOW gel	130	80	[27]
SMB3	0.82	1.48	Present study

future for either removal or recovery of arsenic from aqueous solution contaminated with arsenic. The Langmuir constants (K_L) were 0.11 L/mg for As(V) and 0.07 L/mg for As(III). The Q_m and K_L values were in accordance with trend of the efficiency: As(V) > As(III). These results indicated that the affinity of binding sites on SMB3 surface was in the order: As(V) > As(III). In addition, the data showed that the R_L values decreased with an increase in the C_0 values. The R_L declined from 0.97 to 0.12 for As(V) and from 0.99 to 0.21 for As(III) when the C_0 increased from 0.2 to 60 mg/L, respectively. This parameter ($0 < R_L < 1$) indicates that SMB3 is suitable adsorbent for removal of As(V) and As(III) from aqueous solutions [21].

In comparison, the R^2 values derived from the Freundlich model were 0.941 for As(V) and 0.968 for As(III). The $1/n$ values were 0.56 and 0.81 and the K_F values were 0.18 and 0.04 for As(V) and As(III), respectively. A high value of n suggests a great heterogeneity of surface on the adsorbent [3]. A high value also indicates much favorable adsorption for As(V). These results agreed with the results obtained from the Langmuir model. In addition, ΔG° values were -13.24 kJ/mol for As(V) and -9.29 kJ/mol for As(III), respectively. The negative free energy values indicate the feasibility of the process and the spontaneous nature of adsorption. In addition, high ΔG° values suggest that adsorption might be much spontaneous.

4.5. Effect of pH and mechanism on arsenic adsorption

pH affect on arsenic adsorption is general based on two factors: (i) distribution of arsenic species in solution, and (ii) overall charge of the surface on an adsorbent [12]. Distributions of As(V) and As(III) species are given in Eqs. (8) and (9) based on their corresponding pK_a values [2]:



Therefore, it is important to investigate how pH affects arsenic adsorption on SMB3. The pH values tested ranged from 2.0 to 11.0, and were justified every half hour during the course of adsorption. Fig. 8 shows the effect of pH on arsenic adsorption on SMB3, where the maximum adsorption capacity of As(V) is 0.352 mg/g at pH ~6.0. This may be due to deprotonation of As(V), leading to an increase of adsorption capacity of As(V) with increasing solution pH, thereby strengthening the surface anion exchange process between As(V) and counter ion of chloride on SMB3, which is indicated conceptually by Eqs. (10) and (11). But when the pH values are $>pH_{pzc}$ 6.67, where competition of OH^- for activity sits on SMB3 becomes predominate as OH^- concentration increases, leading to a decrease in adsorption efficiency.

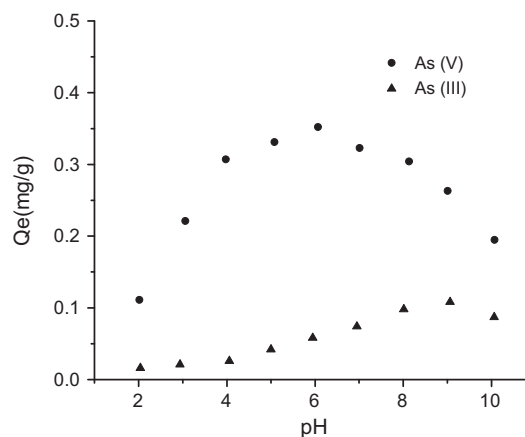
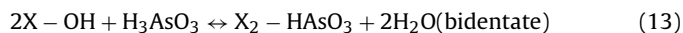
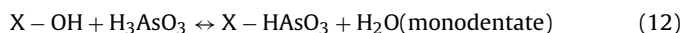


Fig. 8. Effect of pH on As(V) and As(III) adsorption by SMB3. Dose: 10 g/L; background electrolyte: 0.01 M NaCl; equilibration time: 6 h for As(III) and 8 h for As(V); rotary speed: 250 rpm, initial concentration: 5 mg/L and temperature: 33 ± 1 °C.

However, Fig. 8 also shows that the maximum adsorption capacity of As(III) is 0.108 mg/g at pH ~9.0, which is much less than the As(V). This is because of the fact that when initial pH values are <9.0 , the predominant form of As(III) in the solution is H_3AsO_3 , and anion exchange is not a major mechanism as shown by Eqs. (12) and (13), but is a physical adsorption process through Si–O and Al–O groups at the edges of the clay particles [7,30]. The proportion of $H_2AsO_3^-$ increases with increasing solution pH to 9.0, leading to improvement of adsorption efficiency.



where $X \approx Si$ or Al .

4.6. Effect of ionic strength on arsenic adsorption

Investigation of the effect of ionic strength on adsorption is a simple approach to distinguish possible adsorption processes involved either in inner-sphere or outer-sphere surface complexes [8]. The results of the effect of ionic strength on arsenic adsorption on SMB3 showed that the adsorption capacities decreased from 0.449 to 0.062 mg/g for As(V), while the adsorption capacity of As(III) was not significantly affected when the ionic strength increased from 0 to 0.5 M. The adsorption that is not affected by the variations of ionic strength is an inner-sphere complexation; otherwise it is outer-sphere complexes [31]. Hence, the adsorption of As(V) is the outer-sphere complexes through anion exchange, where an increase in ionic strength increases competition of counter ions for adsorption on SMB3, leading to a decrease of the adsorption efficiency of As(V) on SMB3. However, the adsorption of As(III) is mainly physisorption, which predominant forms of As(III) in the solution is H_3AsO_3 , and is inter-sphere complexes through Si–O and Al–O groups at the edges of bentonite particles [30]. Previous studies have also been reported that As(III) adsorption is via the formation of inner-sphere surface complexes while As(V) adsorption is the outer-sphere complexes [18].

4.7. Effect of addition anion on arsenic adsorption

Industrial wastewater often contains a variety of anion species. To check the effects of anions on adsorption arsenic, 0.01 M of chloride, sulfate, fluoride and phosphate ions were therefore added to arsenic solution. Fig. 9 shows the effect of anion addition on the adsorption capacity of As(V) and As(III) on SMB3, where addition of anions hardly affects As(III) adsorption except phosphate,

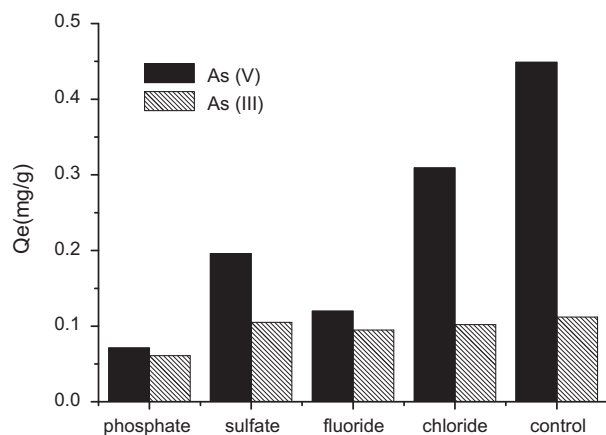


Fig. 9. Effect of major anion on As(V) and As(III) adsorption by SMB3. Dose: 10 g/L; pH: initial pH(8.86); equilibration time: 6 h for As(III) and 8 h for As(V); rotate speed: 250 rpm, initial concentration: 5 mg/L and temperature: $33 \pm 1^\circ\text{C}$.

but suppresses As(V) adsorption. These results agree with previous conclusions which the adsorption of As(V) is the outer-sphere complexes through anion exchange. The tendency of anion effect was in the order: phosphate > sulfate > fluoride > chloride. Phosphate seriously hinders As(V) and As(III) removal, leading to that adsorption capacities of As(V) on SMB3 decreased from 0.449 to 0.071 mg/g and As(III) adsorption efficiency decreased from 0.112 mg/g (when ionic strength was zero) to 0.061 mg/g. The reason could be that phosphate is chemically similar to arsenic [8], which increases competition of arsenic for adsorption sites on the surface of SMB3. Phosphate might also be coordinated with surface functional groups, such as Fe oxides, on the surfaces of SMB3 [32]. As a result, phosphate inhibits the adsorption of arsenic through reducing the availability of adsorption sites, and might also promote the formation of negatively charged surface sites. Therefore, the adsorption of arsenic reduced is attributable to increase the electrostatic repulsion between arsenic and the surface sites of SMB3. Sulfate is divalent that can decrease the thickness of EDL, thereby decreases the adsorption efficiency of As(V) more than fluoride and chloride [33]. The adsorption behavior of As(III) that is unaffected by addition of anions (except phosphate) is an evidence of inner-sphere complex mechanism between As(III) and active sites of the surface of SMB3.

4.8. Regeneration of SMB3

Regeneration of adsorbents is an important practice in environmental remediation. Therefore, 1 g of SMB3 was added to 100 mL of 5 mg/L arsenic solution and mixed until equilibrium in order to determine amount of arsenic to be adsorbed on SBM3. In regeneration tests, 0.5 g of used SMB3 saturated either with As(V) or As(III), was added into 100 mL of either 0.1 M NaOH or 0.1 M HCl solutions for regeneration. The mixer was shaken on a rotary shaker at 200 rpm for 12 h at room temperature. The suspension was filtered and then was analyzed in order to find out how much As(V) was leached out from SMB3. The results showed that desorbed rates were 30.32% for As(V) and 14.72% for As(III), respectively when NaOH solution was used. However, desorbed rates were 74.61% for As(V) and 29.44% for As(III), respectively when HCl solution was used.

5. Conclusions

The results obtained from this work demonstrated that SMB3 could enhance removal of As(III) and As(V) from aqueous solutions. The adsorption capacities of As(III) and As(V) on SMB3 were

5 times higher than those of UB. The adsorption results showed that at initial concentrations of 0.2, 0.5 and 1.0 mg/L, SMB3 could remove As(V) to the level of arsenic below Chinese Environmental Protection guideline values of 50 ppb for treated waste water or 10 ppb for drinking water. The pseudo-second-order model fitted well the adsorption of As(V) and As(III). The maximum adsorption capacity of As(V) calculated from the Langmuir reached as high as 1.48 mg/g, while adsorption capacity of As(III) was 0.82 mg/g. The results derived from effects of pH, ionic strength and addition of anions on arsenic removal indicated that the possible adsorption mechanism of As(V) was the outer-sphere complexes through surface anion exchange, and the possible adsorption mechanism of As(III) was not surface anion exchange but was physisorption intersphere complexes through Si–O and Al–O groups at particle edges of the clay. Finally, desorption rates of SMB3 regenerated using 0.1 M HCl solution were 74.61% and 29.44% for As(V) and As(III), respectively.

Acknowledgements

This work was supported by the Fujian “Minjiang Fellowship” from Fujian Normal University and National Natural Science Foundation of China (20775013).

References

- [1] T.S.Y. Choong, T.G. Chuah, Y. Robiah, F.L. Gregory Koay, I. Azni, Arsenic toxicity, health hazards and removal techniques from water: an overview, *Desalination* 217 (2007) 139–166.
- [2] D. Mohan, C.U. Pittman, Arsenic removal from water/wastewater using adsorbents—a critical review, *J. Hazard. Mater.* 142 (2007) 1–53.
- [3] P. Chutia, S. Kato, T. Kojima, S. Satokawa, Adsorption of As(V) on surfactant-modified natural zeolites, *J. Hazard. Mater.* 162 (2009) 204–211.
- [4] P. Mondal, C.B. Majumder, B. Mohanty, Laboratory based approaches for arsenic remediation from contaminated water: recent developments, *J. Hazard. Mater.* 137 (2006) 464–479.
- [5] A.M. Yusof, N.A.N.N. Malek, Removal of Cr(VI) and As(V) from aqueous solutions by HDTMA-modified zeolite Y, *J. Hazard. Mater.* 162 (2009) 1019–1024.
- [6] P. Chutia, S. Kato, T. Kojima, S. Satokawa, Arsenic adsorption from aqueous solution on synthetic zeolites, *J. Hazard. Mater.* 162 (2009) 440–447.
- [7] B. Dousov, L. Fuitov, T. Grygar, V. Machovic, D. Kolousek, L. Herzogov, M. Lhotka, Modified aluminosilicates as low-cost sorbents of As(III) from anoxic groundwater, *J. Hazard. Mater.* 165 (2009) 134–140.
- [8] A. Ramesh, H. Hasegawa, T. Maki, K. Ueda, Adsorption of inorganic and organic arsenic from aqueous solutions by polymeric Al/Fe modified montmorillonite, *Sep. Purif. Technol.* 56 (2007) 90–100.
- [9] A. Saada, D. Breeze, C. Crouzet, S. Cornu, P. Baranger, Adsorption of arsenic (V) on kaolinite and on kaolinite-humic acid complexes: role of humic acid nitrogen groups, *Chemosphere* 51 (2003) 757–763.
- [10] V. Lenoble, O. Bouras, V. Deluchat, B. Serpaud, J.C. Bollinger, Arsenic adsorption onto pillared clays and iron oxides, *J. Colloid Interface Sci.* 255 (2002) 52–58.
- [11] Z. Li, R.S. Bowman, Retention of inorganic oxyanions by organo-kaolinite, *Water Res.* 35 (2001) 3771–3776.
- [12] D. Borah, S. Satokawa, S. Kato, T. Kojima, Sorption of As(V) from aqueous solution using acid modified carbon black, *J. Hazard. Mater.* 162 (2009) 1269–1277.
- [13] D. Pokhrel, T. Viraraghavan, Arsenic removal from an aqueous solution by a modified fungal biomass, *Water Res.* 40 (2006) 549–552.
- [14] M. Jang, S.H. Min, T.H. Kim, J.K. Park, Removal of arsenite and arsenate using hydrous ferric oxide incorporated into naturally occurring porous diatomite, *Environ. Sci. Technol.* 40 (2006) 1636–1643.
- [15] S. Bang, G.P. Korfiatis, X. Meng, Removal of arsenic from water by zero-valent iron, *J. Hazard. Mater.* 121 (2005) 61–67.
- [16] H. Gen, J.C. Tjell, D. McConchie, O. Schuiling, Adsorption of arsenate from water using neutralized red mud, *J. Colloid Interface Sci.* 264 (2003) 327–334.
- [17] K.G. Bhattacharyya, S.S. Gupta, Adsorption of a few heavy metals on natural and modified kaolinite and montmorillonite: a review, *Adv. Colloid Interface Sci.* 140 (2008) 114–131.
- [18] Z. Li, R. Beachner, Z. McManama, H. Hanlie, Sorption of arsenic by surfactant-modified zeolite and kaolinite, *Micropor. Mesopor. Mater.* 105 (2007) 291–297.
- [19] Y.S. Ho, G. McKay, Pseudo-second order model for sorption processes, *Process Biochem.* 34 (1999) 451–465.
- [20] I. Langmuir, The adsorption of gases on plane surfaces of glass, mica and platinum, *J. Am. Chem. Soc.* 40 (2002) 1361–1403.
- [21] S. Ayoob, A.K. Gupta, P.B. Bhakat, Performance evaluation of modified calcined bauxite in the sorptive removal of arsenic(III) from aqueous environment, *Colloids Surf. A* 293 (2007) 247–254.
- [22] H.M.F. Freundlich, Over the adsorption in solution, *J. Phys. Chem.* 57 (1906) 385.

- [23] Q. Zhou, H.P. He, J.X. Zhu, W. Shen, R.L. Frost, P. Yuan, Mechanism of p-nitrophenol adsorption from aqueous solution by HDTMA⁺-pillared montmorillonite—implications for water purification, *J. Hazard. Mater.* 154 (2008) 1025–1032.
- [24] Y. Xi, R.L. Frost, H. He, Modification of the surfaces of Wyoming montmorillonite by the cationic surfactants alkyl trimethyl, dialkyl dimethyl, and trialkyl methyl ammonium bromides, *J. Colloid Interface Sci.* 305 (2007) 150–158.
- [25] P. Yuan, F. Annabi-Bergaya, Q. Tao, M. Fan, Z. Liu, J. Zhu, H. He, T. Chen, A combined study by XRD, FTIR, TG and HRTEM on the structure of delaminated Fe-intercalated/pillared clay, *J. Colloid Interface Sci.* 324 (2008) 142–149.
- [26] M. Akcay, Characterization and adsorption properties of tetrabutylammonium montmorillonite (TBAM) clay: thermodynamic and kinetic calculations, *J. Colloid Interface Sci.* 296 (2006) 16–21.
- [27] B.K. Biswas, J. Inoue, K. Inoue, K.N. Ghimire, H. Harada, K. Ohto, H. Kawakita, Adsorptive removal of As(V) and As(III) from water by a Zr(IV)-loaded orange waste gel, *J. Hazard. Mater.* 154 (2008) 1066–1074.
- [28] S. Shevade, R.G. Ford, Use of synthetic zeolites for arsenate removal from pollutant water, *Water Res.* 38 (2004) 3197–3204.
- [29] D. Borah, S. Satokawa, S. Kato, T. Kojima, Surface-modified carbon black for As(V) removal, *J. Colloid Interface Sci.* 319 (2008) 53–62.
- [30] A.A. El-Bayaa, N.A. Badawy, E.A. AlKhalik, Effect of ionic strength on the adsorption of copper and chromium ions by vermiculite pure clay mineral, *J. Hazard. Mater.* 170 (2009) 1204–1209.
- [31] K.F. Hayes, C. Papeis, J.O. Leckie, Modeling ionic strength effects on anion adsorption at hydrous oxide/solution interfaces, *J. Colloid Interface Sci.* 125 (1988) 717–726.
- [32] K.H. Goh, T.T. Lim, Geochemistry of inorganic arsenic and selenium in a tropical soil: effect of reaction time, pH, and competitive anions on arsenic and selenium adsorption, *Chemosphere* 55 (2004) 849–859.
- [33] C.H. Weng, Y.C. Sharma, S.H. Chu, Adsorption of Cr(VI) from aqueous solutions by spent activated clay, *J. Hazard. Mater.* 155 (2008) 65–75.